ADVANCED FUNCTIONAL MATERIALS
www.afm-journal.de

Highly Transparent and Conductive Stretchable Conductors Based on Hierarchical Reticulate Single-Walled Carbon Nanotube Architecture

*Le Cai, Jinzhu Li, Pingshan Luan, Haibo Dong, Duan Zhao, Qiang Zhang, Xiao Zhang, Min Tu, Qingsheng Zeng, Weiya Zhou, and Sishen Xie**

Free-standing, hierarchical reticulate single-walled carbon nanotube (SWCNT) films are embedded in poly(dimethylsiloxane) (PDMS) to fabricate stretchable conductors (SWCNT/PDMS stretchable conductors). The stretchable conductors are highly transparent in visible light region and retain excellent conductance under large tensile strains. Strain tests reveal a unique strain-history dependence behavior of the resistance, and resistance stabilization is achieved upon repetitive stretching and releasing, implying that the SWCNT/PDMS stretchable conductors can be programmed to be reversibly stretched to a defined strain without resistance changes. A quantitative description of the increase in resistance is determined by adopting the Weibull distribution. Moreover, a light-emitting diode is illuminated using a repetitively stretched SWCNT/PDMS strip as the connecting wire, demonstrating the utility of the stretchable conductors as interconnects for stretchable electronics. Because of the high transparency, high conductivity, and excellent stretchability, in addition to the facile fabrication, the SWCNT/PDMS stretchable conductors might be widely used as interconnects and electrodes for stretchable intelligent and functional devices.

1. Introduction

Future electronics should be not only miniatured but also soft, flexible, stretchable and curvilinear.[1] Devices that retain good functionality under stretching are essential for many applications such as medical implements, skin-like sensors, wearable electronics, structural health monitoring and other areas requiring stretchability and conformability.[2] Recently, the developments in stretchable electronics have attracted extensive research interests and substantial progress has been made. Generally, two conceptually distinct but complementary scenarios are being developed. One relies on the new structural layouts of conventional materials.[3] Conventional semiconductors and metals are fabricated into wavy shapes or herringbone configurations on an elastomeric substrate. The applied strains are accommodated by the changes in the wavelengths and amplitudes of the wavy structures, similar to the mechanics of an accordion bellows. Conformal integrated circuits, eyeball digital camera and stretchable inorganic light-emitting diode (LED) display have been demonstrated through this pathway.[4–6] The other is to exploit novel materials, including carbon nanotubes, graphene and intrinsically conducting polymers and great achievements have been made through this pathway.[7] Ajayan el al. fabricated flexible coducting compoites using aligned multiwall carbon naontube arrays and explored their utility as flexible field-emission devices.[8] Several other stretchable devices have also been demonstrated, including stretchable capacitors,[9] Mg batteries,[10] solar cells,[11] skin-like sensor,[12] light-emitting elements,[13–15] and dielectric elastomer actuator.[16]

Stretchable interconnects and electrodes that can maintain substantial electrical conductance under strain are crucial for the realization of stretchable electronics. Stretchable conductors have been demonstrated by several groups through either of the above routes.[17–25] By virtue of their 1D attributes, high electrical conductivity, transparency, robustness and electrochemical activities, carbon nanotubes are ideal material to fabricate stretchable interconnects and electrodes. Several kinds of stretchable conductors have been reported in literature based on carbon nanotubes. Single-walled carbon nanotubes (SWCNTs) were mixed with an ionic liquid and a fluorinated copolymer matrix to form rubber-like conductors.[22] Aligned multiwalled carbon nanotube (MWCNT) ribbons were embedded in an elastomer to form transparent stretchable conductors.[21]

L. Cai, J. Z. Li, P. S. Luan, H. B. Dong, D. Zhao, Q. Zhang, X. Zhang, M. Tu, Prof. W. Y. Zhou, Prof. S. S. Xie
Beijing National Laboratory for Condensed Matter Physics
Institute of Physics
Chinese Academy of Sciences, Beijing 100190, China
E-mail: ssxie@aphy.iphy.ac.cn
L. Cai, J. Z. Li, P. S. Luan, H. B. Dong, D. Zhao, Q. Zhang, X. Zhang, M. Tu
Graduate School of the Chinese Academy of Sciences
Beijing 100049, China
Q. S. Zeng
Key Laboratory for the Physics and Chemistry of Nanodevices
Department of Electronics
Peking University
Beijing, 100871, China

DOI: 10.1002/adfm.201201013

Another kind of transprent stretchable conducotrs were fabricated by embedding cross-stacked superaligned carbon nanotube films in an elastomer.[24] In another report, elastomeric conductive composites were fabricated by infiltrating MWCNT forests with polyurethane, showing extremely high elasticity (1400% strain).[18] A recent study reported a kind of stretchable conductors by buckling CNT ribbons to form wavy structures while releasing the prestrained elastomer substrates.[23] By coating the CNT with a thin layer of Au/Pd alloy, fairly high electrical conductance was obtained. Very recently, Zhu et. al proposed a new strategy to fabricate transparent stretchable conductors by buckling aligned carbon nanotubes via a stretching/releasing step after the device manufacturing.[25] Nevertheless, it is still a challenge to fabricate stretchable conductors with high transparency, high conductivity and excellent stretchability through a simple and easy route.

Here, we report the fabrication of highly transparent stretchable conductors by embedding hierarchical SWCNT films in poly(dimethylsiloxane) (PDMS) (hereafter defined as SWNCT/PDMS for convenience). Compared with the reported stretchable conductors, our SWCNT/PDMS films inherit the superior electrical conductivity of the pristine SWCNT films (≈2000 S cm^{-1}) and maintain stable conductance upon repetitive stretching to large tensile strains. The high transparency, superior conductivity and stretchability, as well as the facile fabricating method, will ensure wide applications of our SWCNT/PDMS composites in stretchable electronics and optoeletronics.

2. Results and Discussion

2.1. Fabrication of SWCNT/PDMS Stretchable Conductors

The free-standing SWCNT films were directly synthesized via a floating catalyst chemical vapor deposition (FCCVD) method.[26,27] Due to the unique hierarchical reticulate structure and very long and good interbundle connects (shown in **Figure 1**) formed during the growth process at elevated temperatures, our SWCNT films owns excellent electrical and mechanical properties: the electrical conductivity and mechanical strength can reach 2000 S cm^{-1} and 350 MPa, respectively. Hierarchical reticulate structure is most effective for electrical and mechanical transport. For millions of years, nature has employed such structure as the veins of leaves to transport nutrient substance (see insets of Figure 1). By adjusting the growth conditions, such as the sublimation rates of catalysts and deposition time, we can obtain films with different thicknesses, thus expected transmittances. The transmittances in visible region evolve from 20% to 70% while the film thicknesses decrease from 500 nm to 100 nm.[26] Our previous studies have demonstrated that this kind of SWCNT films are ideal materials for high strength fiber,[28] mechanical reinforced composites,[29,30] saturable absorbers,[31] and electrodes for electrochemical supercapacitors and non-aqueous ultrafast artificial muscles.[32,33]

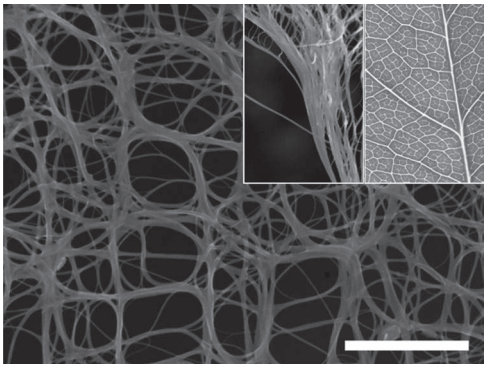

Figure 1. SEM images of the as-grown single walled carbon nanotube films. It can be clearly seen that the carbon nanotube bundles entangle randomly to form a reticulate structure. The scale bar represents 500 nm. The insets show the comparison of the hierarchical reticulate structure features of the SWCNT film (left inset) and the leaf veins (right inset).

The fabrication process of the stretchable SWCNT/PDMS films is illustrated in **Figure 2**a. First, as-grown SWCNT films were immersed in 10 M HNO_3 to remove impurities and introduce hydrophilic groups (e.g., —COOH) to the side walls of SWCNTs.[9] The mechanical robustness of SWCNT films remained intact while the sheet condcutance was improved by a factor of 3, probably originating from the doping effect of HNO_3.[34] Oxygen plasma treatments were adopted to modify the hydrophobic PMDS surface with hydrophilic functionalities.[35] These pretreatments could ensure tight contacts between SWCNT films and PDMS through condensation reactions of the hydrophilic functionalities. Then, the treated SWCNT films were laid onto the hydrophilic PDMS surfaces and flattened using distilled water. After the water vaporized, the adhesion forces between the SWCNT films and the PDMS surfaces were strong enough to bear repetitive scratching. Next, the SWCNT/PDMS films were cut into strips with dimensions of 20 mm × 3 mm. Electrical electrodes were then fabricated at the two ends of the strips. After that, uncured PDMS was casted onto the SWCNT side and the whole sample was baked in an oven at 100 °C for 1 h to cure the top PDMS.

Similar embedment procedures have been reported in literature.[21,24] This fabrication method is very simple and environmental friendly, because prestrain and additive, such as ionic liquid, are not involved. Moreover, this polymer embedding method does not destroy the intrinsic transport network of SWCNTs, thus is very suitable for our free-standing reticulate SWCNT films. The prepared SWCNT/PDMS films are very flexible and can be reversibly bended and twisted without structural damages, as shown in Figure 2b,c. Because of the nanoscale thicknesses of the original SWCNT film, the SWCNT/PDMS composite films own high transparency in the visible region (Figure 2d,e). The transmittance is as high as 80% at 550 nm for the composite film shown in Figure 2d. The sheet resistance of the unstrained SWCNT/PDMS films was estimated to be in the same order with the HNO_3 treated SWCNT films, indicating that the embedding process does not deteriorate the electrical conductivity of the SWCNT films.

2.2. Stretchability of SWCNT/PDMS Stretchable Conductors

Figure 3a presents the changes in resistance ($\Delta R/R_0$, R_0 is the original resistance of the as-prepared sample) of a typical

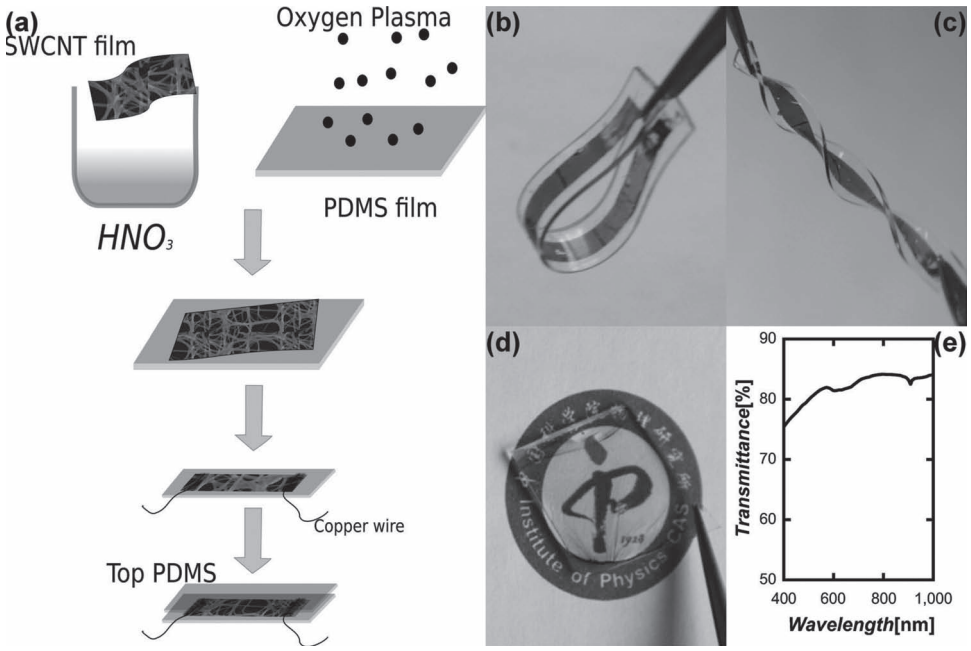

Figure 2. a) Schematic illustration of the procedures to prepare SWCNT/PDMS stretchable conductors. b,c) Digital photographs of a bended and twisted SWCNT/PDMS stretchable conductor, showing their flexibility. Here, the samples look opaque because fairly thick SWCNT films were used. d) Digital photograph of a transparent SWCNT/PDMS film. e) The transmittance spectra of the SWCNT/PDMS film shown in d).

SWCNT/PDMS strip under repetitive stretching and releasing with a strain of 40% (at a speed of 10% s^{-1}). Except for the steep rising in the initial cycles, the resistance kept stable until mechanical fracture after 500 cycles. The superior electrical conductance of our SWCNT films mainly originated from the strong interbundle junctions.[26] It is thus reasonable to attribute the increases in resistance to the loss of interbundle junctions. After a conditioning stage of about 20 cycles, no further junction break was induced and a stabile morphology of the nanotube network was achieved, leading to the conductance stabilization.

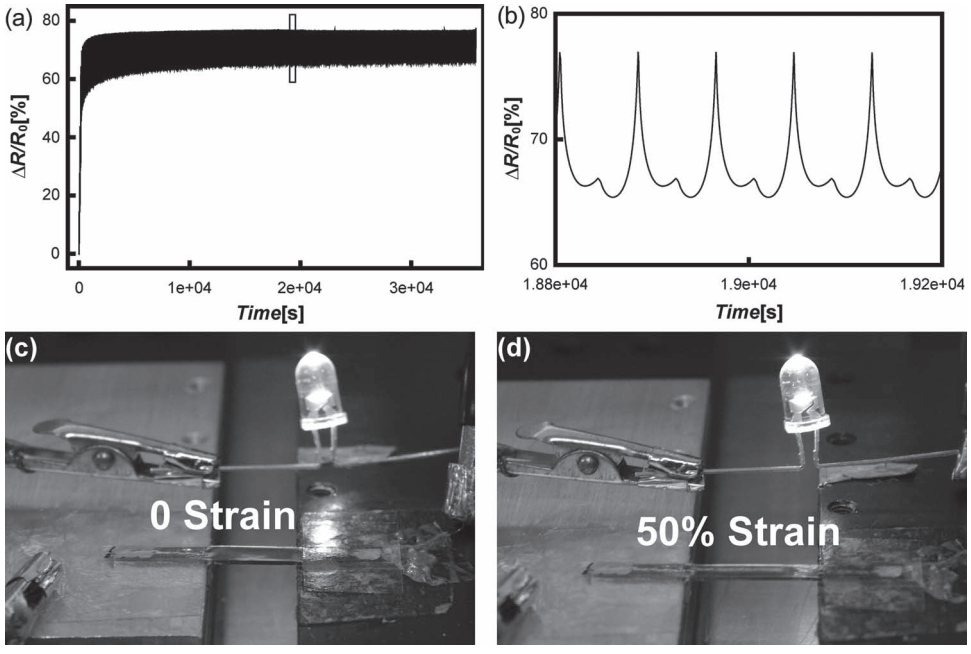

Figure 3. a) $\Delta R/R_0$ curve in about 500 cycles of stretching and releasing with a strain of 40%. b) A close look at four stable cycles. Enlargements of the parts enclosed in the rectangle in (a). c,d) Digital pictures of an LED illuminated using a SWCNT/PDMS strip as the connecting wire, where the strains applied to the strips are 0 and 50%, respectively.

Because of the excellent conductivity of the as-prepared sample, the stabilized resistance was still rather low ($\Delta R/R_0$ = 65% at $\varepsilon = 0$). A close look at four stabilized cycles is given in Figure 3b. An unexpected minor peak was observed in the vicinity of zero strain. This minor peak is speculated to result from the reduction (due to the Poisson effect) of overlapping lengths (through which electrons can tunnel and contribute to the entire conductance) between adjacent nanotube bundles. The reduction of overlapping lengths will suppress the electronic tunneling thus the entire conductance. SEM observations (see Figure S1 in Supporting Information) on neat SWCNT films reveal that, upon stretching, randomly distributed nanotube bundles are preferentially aligned along the tensile direction, leading to larger overlapping lengths and closer distances between adjacent bundles. The same scenario is believed to unfold in the case of stretchable conductors, although direct observation is not available at the moment.

As a proof-of-principle demonstration for stretchable electronics, we used an as-prepared SWCNT/PDMS stretchable conductor as connecting wire to illuminate a commercial light-emitting diode (LED, turn on voltage 2.5 V; Figure 3c,d). The stretchable conductor worked well under repetitively stretching with a 50% strain (see Movie S1 in Supporting Information).

A remarkable strain history-dependent feature of the resistance (as shown in **Figure 4**a) was observed when the sample was subjected to consecutive stretching and releasing cycles: 0 → 10%→0 → 20%→0 → 30%→0 → 40%→0 → 50%→0 → 60%. Following every loading stage and unloading stage, the applied strain was held for 50 s. At the first loading stage (10% strain), $\Delta R/R_0$ increased from 0 to 5%. When the strain was released, $\Delta R/R_0$ decreased nonlinearly until the strain returned to 5%, and kept constant (about 1%) afterwards (as shown in the inset). The recoverable increase in resistance was attributed to the elastic elongation of nanotubes and interbundle junctions. In the next loading process, $\Delta R/R_0$ almost retraced the curve of last releasing process until the previous maximum strain (10%) was approached, after which $\Delta R/R_0$ rose linearly up to 19%. In the following unloading stage, $\Delta R/R_0$ decreased nonlinearly to 7% and kept constant after 10% strain was restored. Similar behaviors were observed in the following cycles: when the strain was loaded, a flat region, a nonlinear region and a linear slope came out successively, while in the unloading stage, a nonlinear region was followed by a plateau. More interbundle junctions would break once the applied strain exceeded the previous maximum, resulting in the linear slope region and a higher plateau, which is responsible for the strain-history dependent feature. Except for junction breaks, stretching would also elongate the nanotubes, diminish the interbundle contact areas and depart touching (but not in conjunction) nanotube segments between which electrons can tunnel, which is responsible for the nonlinear regions. The sample fractured at ε = 60% and $\Delta R/R_0$ = 125%, indicating the elasticity limits of our samples are determined by the polymer matrix and better endurance can be achieved by optimizing the polymer matrix.

Similar strain-history dependent behaviors have been reported in literature.[12,25] The dependence of resistance on the strain history implies that our sample can be programmed (by the first cycle) to be reversibly stretched with no noticeable

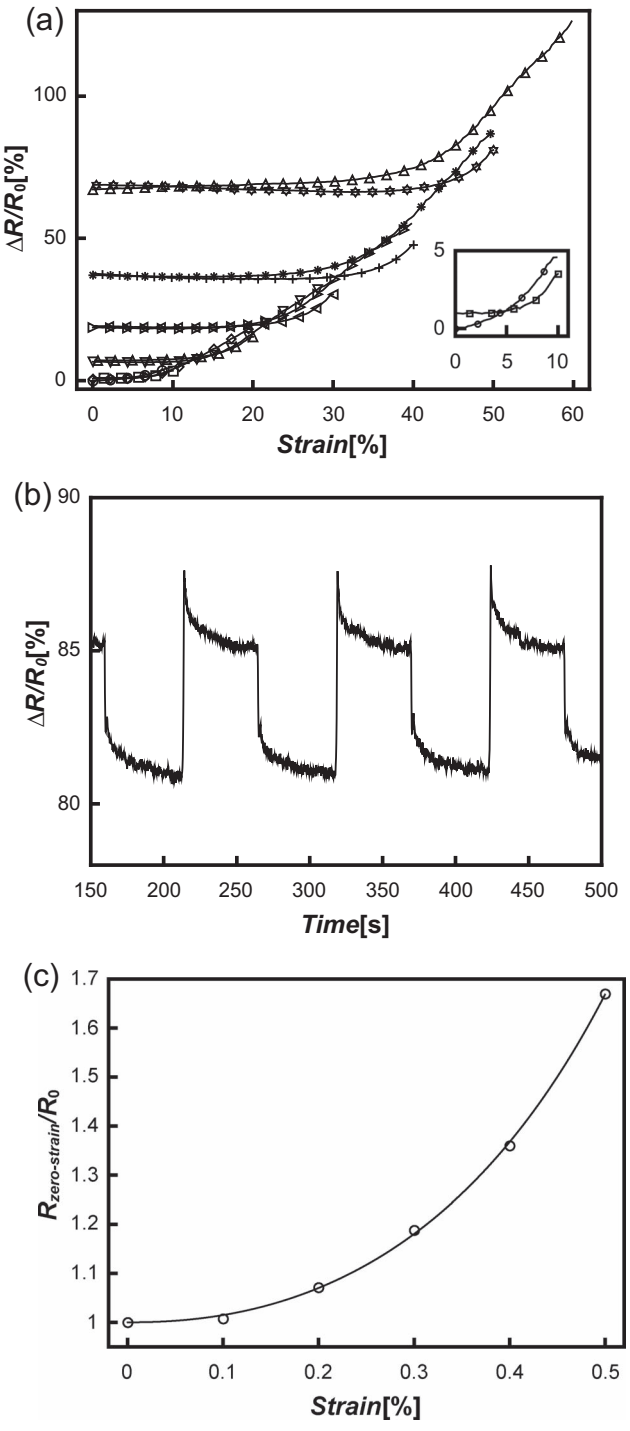

Figure 4. a) Typical $\Delta R/R_0$ vs. strain curves in six successive loading-unloading cycles, revealing the dependence of $\Delta R/R_0$ on the strain history. Inset: A close look at the first loading-unloading cycle. b) Four cycles of stretching and releasing with a previous maximum strain of 50%. c) Normalized zero-strain resistance (normalized to the resistance of the as-prepared strip, $R_{\text{zero-strain}}/R_0$) of a SWCNT/PDMS stretchable conductor versus the applied maximum strains (labeled on the horizontal axis). Open dots are experimental data and solid lines are fitting curves in (c).

change in resistance in a defined strain range. Figure 4b shows three cycles with a strain of 50% (the strain was held for 50 s on every stage), where the resistance reversibly increased by less than 10%. The resistance responded to strain almost instantly, although remarkable creeping behavior appeared (with overshoots of about 3% and a recovery time of more than 50 s), resulting from the viscoelasticity of PDMS.

In Figure 4c, we show the normalized zero-strain resistance ($R_{\text{zero-strain}}/R_0$, $R_{\text{zero-strain}}$ corresponds to the plateau region and R_0 is the resistance of the as-prepared sample) as a function of the applied maximum strain (labeled on the horizontal axis). In order to better understand the strain-history dependence, we employ the Weibull distribution to find a quantitative description of the $R_{\text{zero-strain}}/R_0$ curve. Weibull distribution, named after Waloddi Weibull, is widely applied to reliability and failure analysis, weather forecasting, general insurance and hydrology.[36] According to Weibull distribution, the broken probability of each fiber in a bundle can be expressed as

$$P(\varepsilon) = 1 - e^{-L(\varepsilon/\varepsilon_0)^{\beta}} \quad (1)$$

where ε is the applied strain, ε_0 the characteristic strain, L a dimensionless factor, and β the shape factor.

Considering its wide applications, we tentatively apply Weibull distribution to our SWCNT/PDMS films. In the case of our stretchable conductors, Equation (1) can describe the broken probability of one interbundle junction. Regarding that the resistance increase is mainly caused by junction breaks, we assume that the zero-strain conductance (plateau region) is proportional to the number of intact junctions, thus the ratio $R_{\text{zero-strain}}/R_0$ will be (see Supporting Information for details)

$$R_{\text{zero-strain}}/R_0 = e^{L(\varepsilon/\varepsilon_0)^{\beta}} \quad (2)$$

Owing to the binding effect of PDMS molecules, the value of L for the composite films should be smaller than that for the neat SWNCT films.[26] Herein, we set L to be 500. Then, we can obtain very good fitting to the experimental data (as shown in Figure 4c), with the values of ε_0 and β being 11.3 and 2.21, respectively. Despite of the the simplification of the model, the above results can provide heuristic information. The values of ε_0 and β for the SWCNT/PDMS films are very different from those for the neat SWCNT films,[26] implying that PDMS molecules significantly affect the mechanical properties of the nanotube films. On one hand, the surprisingly large value of ε_0 means that the SWCNT/PDMS films can be potentially stretched to a very large strain. On the other hand, the introduction of PDMS causes great broadening of the strength distribution, as inferred from the small value of β. Based on the above consideration, by optimizing the composite configuration, the potential stretchability of our SWCNT/PDMS films can be fully realized.

2.3. Advantages and Challenges of SWCNT/PDMS Stretchable Conductors

Available strain limits of stretchable condcutors are crucial for their designs and applications. The fracture strain of our SWCNT/PDMS stretchable conductors is up to 60%. Although this value is much lower than that of pure PDMS, it is much higher that of neat SWCNT films (only about 10%).[26] When the neat film is subjected to a tensile strain, following the continuous and uniform deformation of the mesh, stress concentrations occur at preexisting micro cracks. Enlargements of the micro cracks cause further stress concentrations and the appearance of macro cracks, i.e., the final fracture of the whole film. Whereas in the composite, the molecular coupling between polymer molecules and SWCNTs effectively mitigates the stress concentrations.[26] More importantly, the introduction of polymer matrix can maintain the structural integrity of the carbon nanotube networks even if lots of junctions break up at high strain levels. On the other hand, due to the firm interbundle connects and hierarchical structure in our films, tensile strains are mainly accommodated by the free deformations of the nanotube mesh and the breaks of weak junctions, leaving the other junctions intact, thus maintaining excellent electrical conductance. So, we believe the superior stretchability of SWCNT/PDMS stretchable conductors results from the combination of the 1D attributes of nanotubes, the good interbundle contacts and unique hierarchical structure of our SWCNT films as well as the good elasticity of PDMS. It should be noted that, although we attributed the resistance increase to the junction breaks, intertube sliding (sliding between CNTs) may also occur as a result of the sliding between the CNTs and the PDMS substrate, which could also contribute to the resistance increase.[21,25] Nevertheless, morphological characterizations were not feasible as a result of embedment.

High optical transmittance and low sheet resistance are both essential for the utility as electrodes in optoelectronic applications. Our SWCNT/PDMS composite films exhibit very low sheet resistance while the transparency can be varied in a wide range. **Figure 5**a) presents the transmittance spectra in the range of 400–1000 nm of several composite films with different unstrained sheet resistance. The transmittance at 550 nm is about 62% for a composite film with sheet resistance of 53 Ω $\square^{-1}$, 52% for 20 Ω $\square^{-1}$, 48% for 18 Ω $\square^{-1}$, 38% for 14 Ω $\square^{-1}$ and 16% for 7 Ω $\square^{-1}$. Several other kinds of transparent stretchable conductors have been reported based on carbon nanotubes in literature.[17–25] In Figure 5b, we show a comparison of our SWCNT/PDMS composite films with the reported results. It can be seen that our SWCNT/PDMS composite films are among the best results regarding both optical transmittance and electrical conductance.

We stress that our SWCNT/PDMS composites are definitely not limited to the utility as interconnects for stretchable electronics. Due to the superior conductivity, good tranparency and large surface area of the SWCNT films, the SWNCT/PDMS composites are prominent candidates to fabricate stretchable functional devices. For example, they can be used as electrodes for stretchable solar cells, stretchable light-emitting elements, stretchable electrochromic devices and stretchable actuators. In addition, if the SWCNT films are modified with electrochemical active polymers or oxides before embedding in PDMS, they will be ideal materials to fabricate stretchable supercapacitors and batteries.[33,37] Nevertheless, the potential stretchability of SWCNT/PDMS composites has not been fully realized, since the fracture strain is significantly lower than that of pure PDMS. A better stretchability can be obtained by thinning the SWCNT films or introducing new energy dissipation mechanisms, e.g., replacing the thermal set PDMS with a thermal plastic elastomer (TPE).

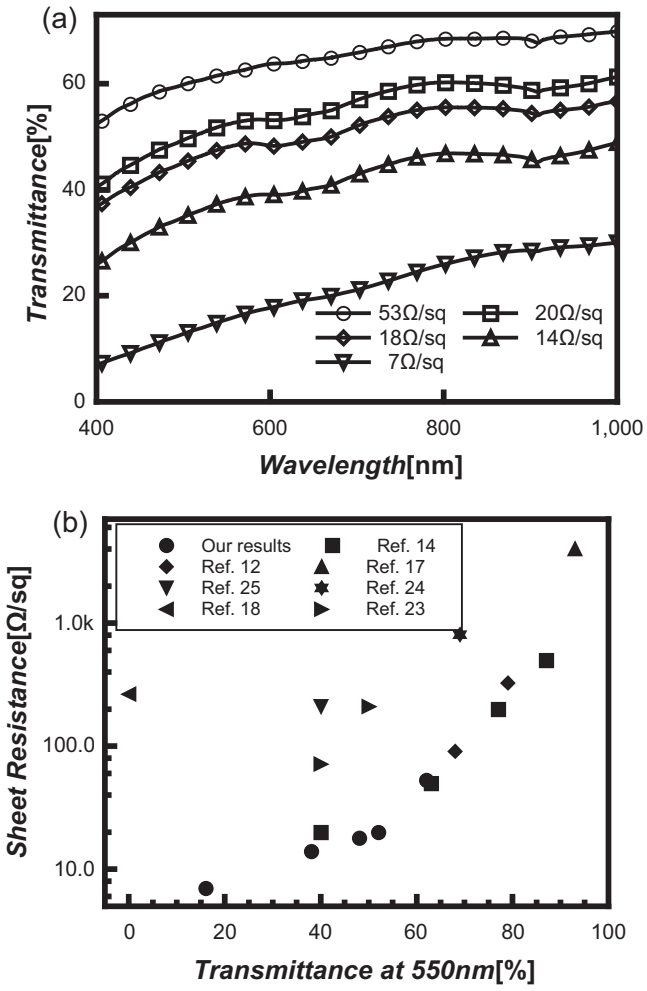

Figure 5. a) Transmittance spectra in the range of 400–1000 nm for five SWCNT/PDMS composite films with sheet resistance specified. b) A comparison between the composite film and the results reported in literature, regarding the sheet resistance and transmittance at 550 nm. In ref. [18] the samples were non-transparent; in ref. [23] the sheet resistance was 211 $\Omega\ \square^{-1}$ and 72 $\Omega\ \square^{-1}$ before and after sputtering Au/Pd alloy, respectively. The transmittance was estimated from the digital picture in the paper; in ref. [24] the sheet resistance was that of the pure two-layer cross-stacked carbon nanotube film, which would increase after embedding with PDMS.

3. Conclusions

In summary, highly conductive hierarchical SWCNT films were embedded in PDMS to fabricate stretchable conductors with high transparency, excellent electrical conductance and good elasticity. Their stretchability was investigated by monitoring the changes in resistance under cyclic strain tests. The results show that our SWCNT/PDMS stretchable conductors retain excellent electrical conductance upon repetitive stretching to a large strain. The increases in resistance were mainly attributed to the breaks of interbundle junctions induced by the applied tensile strains. Weibull distribution was employed to quantitatively describe the resistance increase of the SWCNT/PDMS stretchable conductors. The stretchable conductors can be programmed by the initial stretching cycles to be reversibly stretched to a large strain without noticeable resistance increase, which is essential for the utility as interconnects of stretchable electronics. We have also demonstrated that it is feasible to use our SWCNT/PDMS stretchable conductors as connecting wires for stretchable electronics. Since the stretchability and endurance of the SWCNT/PDMS composite films are limited by the polymer matrix, better performances can be obtained by optimizing the elastomer matrix. Furthermore, because the reported SWCNT/PDMS stretchable conductors are highly transparent and stretchable and easy to fabricate, they will be widely used not only as interconnects but also as electrodes for many intelligent electronics, such as stretchable energy storage devices, optoelectronic devices and so on.

4. Experimental Section

Synthesis of SWCNT Films: The SWCNT films used in this study were synthesized via a floating catalyst chemical vapor deposition (FCCVD) method. Experimental details can be found in our early studies[26]. Methane was used as carbon source. The deposition temperature was 1050–1100 °C. A mixture of sulfur and ferrocene was used as catalyst. By adjusting the growth conditions, such as the deposition time and sublimation temperature of catalyst, SWCNT films with desired thicknesses can be obtained.

Preparation of PDMS Film: Silicon gel (Sylgard 184, Dorcorning) were mixed with cross linker (weight ratio 10:1), poured into a mould and cured at 100 °C for 1 h.

Fabrication of SWCNT/PDMS Composites: First, the as-grown SWCNT films were immersed in HNO_3 (10 M) for 48 h. Oxygen plasma (100 W, 10 min) treatments were adopted to modify the hydrophobic PMDS surface with hydrophilic functionalities.[35] Then, the treated SWCNT films were laid onto the hydrophilic PDMS surfaces and flattened using distilled water. Next, the SWCNT/PDMS films were cut into strips with dimensions of 20 mm × 3 mm. Copper wires were then pasted to the SWCNT film side at the two ends of the strips with silver paste. After that, uncured PDMS was casted onto SWNCT side and the whole sample was baked in an oven at 100 °C for 1 h to cure the top PDMS.

Characterization Methods: Repetitive strain tests were performed using a homemade one-dimensional motorized tensile stage equipped with a micrometer (minimum moving step, 0.1 μm). The SWCNT/PDMS strips were fixed on the stage, with the central part (gauge length, 10 mm) being stretched. Meanwhile, the resistance was measured using a Keithley 2400 multimeter through a two-probe method. The whole system was controlled by a computer through a LabVIEW program.

Stress-strain curves were obtained using a TA Instruments Dynamic Mechanical Analyzer Q800. The absorption spectra were recorded by a UV-vis-NIR spectrophotometer (Varian Cary 5000). SEM observations were carried out using a HiTachi S5200 field emission scanning electron microscopy (FESEM) system.

Supporting Information

Supporting Information is available from the Wiley Online Library or from the author.

Acknowledgements

This work is supported by the National Basic Research Program of China (Grant No. 2012CB932302), the National Natural Science Foundation of China (51172271, and 90921012) and Beijing Municipal Education Commission (Grant No. YB20108000101).

Received: April 10, 2012
Revised: June 4, 2012
Published online: August 1, 2012

[1] J. A. Rogers, Y. Huang, *Pro. Natl. Acad. Sci. USA* **2009**, *106*, 10875.
[2] J. A. Rogers, T. Someya, Y. Huang, *Science* **2010**, *327*, 1603.
[3] D.-H. Kim, J. Xiao, J. Song, Y. Huang, J. A. Rogers, *Adv. Mater.* **2010**, *22*, 2108.
[4] D.-H. Kim, J.-H. Ahn, W. M. Choi, H.-S. Kim, T.-H. Kim, J. Song, Y. Y. Huang, Z. Liu, C. Lu, J. A. Rogers, *Science* **2008**, *320*, 507.
[5] H. C. Ko, M. P. Stoykovich, J. Song, V. Malyarchuk, W. M. Choi, C.-J. Yu, I. I. I. J. B. Geddes, J. Xiao, S. Wang, Y. Huang, J. A. Rogers, *Nature* **2008**, *454*, 748.
[6] S.-I. Park, Y. Xiong, R.-H. Kim, P. Elvikis, M. Meitl, D.-H. Kim, J. Wu, J. Yoon, C.-J. Yu, Z. Liu, Y. Huang, K.-c. Hwang, P. Ferreira, X. Li, K. Choquette, J. A. Rogers, *Science* **2009**, *325*, 977.
[7] T. Sekitani, T. Someya, *Adv. Mater.* **2010**, *22*, 2228.
[8] Y. J. Jung, S. Kar, S. Talapatra, C. Soldano, G. Viswanathan, X. S. Li, Z. L. Yao, F. S. Ou, A. Avadhanula, R. Vajtai, S. Curran, O. Nalamasu, P. M. Ajayan, *Nano Lett.* **2006**, *6*, 413.
[9] C. Yu, C. Masarapu, J. Rong, B. Wei, H. Jiang, *Adv. Mater.* **2009**, *21*, 4793.
[10] C. Wang, W. Zheng, Z. Yue, C. O. Too, G. G. Wallace, *Adv. Mater.* **2011**, *23*, 3580.
[11] D. J. Lipomi, B. C. K. Tee, M. Vosgueritchian, Z. Bao, *Adv. Mater.* **2011**, *23*, 1771.
[12] D. J. Lipomi, M. Vosgueritchian, B. C. K. Tee, S. L. Hellstrom, J. A. Lee, C. H. Fox, Z. Bao, *Nat. Nanotechnol.* **2011**, *6*, 788.
[13] T. Sekitani, H. Nakajima, H. Maeda, T. Fukushima, T. Aida, K. Hata, T. Someya, *Nat. Mater.* **2009**, *8*, 494.
[14] Z. Yu, X. Niu, Z. Liu, Q. Pei, *Adv. Mater.* **2011**, *23*, 3989.
[15] Z. Yu, Q. Zhang, L. Li, Q. Chen, X. Niu, J. Liu, Q. Pei, *Adv. Mater.* **2011**, *23*, 664.
[16] W. Yuan, L. Hu, Z. Yu, T. Lam, J. Biggs, S. M. Ha, D. Xi, B. Chen, M. K. Senesky, G. Gruner, Q. Pei, *Adv. Mater.* **2008**, *20*, 621.
[17] K. H. Kim, M. Vural, M. F. Islam, *Adv. Mater.* **2011**, *23*, 2865.
[18] M. K. Shin, J. Oh, M. Lima, M. E. Kozlov, S. J. Kim, R. H. Baughman, *Adv. Mater.* **2010**, *22*, 2663.
[19] X. Wang, H. Hu, Y. Shen, X. Zhou, Z. Zheng, *Adv. Mater.* **2011**, *23*, 3090.
[20] H.-B. Yao, G. Huang, C.-H. Cui, X.-H. Wang, S.-H. Yu, *Adv. Mater.* **2011**, *23*, 3643.
[21] Y. Zhang, C. J. Sheehan, J. Zhai, G. Zou, H. Luo, J. Xiong, Y. T. Zhu, Q. X. Jia, *Adv. Mater.* **2010**, *22*, 3027.
[22] T. Sekitani, Y. Noguchi, K. Hata, T. Fukushima, T. Aida, T. Someya, *Science* **2008**, *321*, 1468.
[23] F. Xu, X. Wang, Y. T. Zhu, Y. Zhu, *Adv. Funct. Mater.* **2012**, *22*, 1279.
[24] K. Liu, Y. H. Sun, P. Liu, X. Y. Lin, S. S. Fan, K. L. Jiang, *Adv. Funct. Mater.* **2011**, *21*, 2721.
[25] Y. Zhu, F. Xu, *Adv. Mater.* **2012**, *24*, 1073.
[26] W. Ma, L. Song, R. Yang, T. Zhang, Y. Zhao, L. Sun, Y. Ren, D. Liu, L. Liu, J. Shen, Z. Zhang, Y. Xiang, W. Zhou, S. Xie, *Nano Lett.* **2007**, *7*, 2307.
[27] L. Song, L. Ci, L. Lv, Z. P. Zhou, X. Q. Yan, D. F. Liu, H. J. Yuan, Y. Gao, J. X. Wang, L. F. Liu, X. W. Zhao, Z. X. Zhang, X. Y. Dou, W. Y. Zhou, G. Wang, C. Y. Wang, S. S. Xie, *Adv. Mater.* **2004**, *16*, 1529.
[28] W. Ma, L. Liu, R. Yang, T. Zhang, Z. Zhang, L. Song, Y. Ren, J. Shen, Z. Niu, W. Zhou, S. Xie, *Adv. Mater.* **2009**, *21*, 603.
[29] J. Li, Y. Gao, W. Ma, L. Liu, Z. Zhang, Z. Niu, Y. Ren, X. Zhang, Q. Zeng, H. Dong, D. Zhao, L. Cai, W. Zhou, S. Xie, *Nanoscale* **2011**, *3*, 3731.
[30] W. Ma, L. Liu, Z. Zhang, R. Yang, G. Liu, T. Zhang, X. An, X. Yi, Y. Ren, Z. Niu, J. Li, H. Dong, W. Zhou, P. M. Ajayan, S. Xie, *Nano Lett.* **2009**, *9*, 2855.
[31] W. Ma, B. Feng, Y. Ren, Q. Zeng, Z. Niu, J. Li, X. Zhang, H. Dong, W. Zhou, S. Xie, *J. Nanosci. Nanotechnol.* **2010**, *10*, 7333.
[32] J. Li, W. Ma, L. Song, Z. Niu, L. Cai, Q. Zeng, X. Zhang, H. Dong, D. Zhao, W. Zhou, S. Xie, *Nano Lett.* **2011**, *11*, 4636.
[33] Z. Niu, W. Zhou, J. Chen, G. Feng, H. Li, W. Ma, J. Li, H. Dong, Y. Ren, D. Zhao, S. Xie, *Energ. Environ. Sci.* **2011**, *4*, 1440.
[34] J. L. Blackburn, T. M. Barnes, M. C. Beard, Y. H. Kim, R. C. Tenent, T. J. McDonald, B. To, J. Coutts, M. J. Heben, *ACS Nano* **2008**, *6*, 1266.
[35] D. Bodas, C. Khan-Malek, *Microelectron. Eng.* **2006**, *83*, 1277.
[36] Weibull distribution, http://en.wikipedia.org/wiki/Weibull_distribution (July 2012).
[37] A. Goyal, A. L. M. Reddy, P. M. Ajayan, *Small* **2011**, *7*, 1709.